Journal of Organometallic Chemistry, 364 (1989) 105–117
Elsevier Sequoia S.A., Lausanne – Printed in The Netherlands
JOM 09532

Synthesis and structural characterization of group 4 *ansa*-metallocene complexes containing a 1-sila-3-metallacyclobutane ring

Ashok Kabi-Satpathy, Chandrasekhar S. Bajgur, Karuna P. Reddy, and Jeffrey L. Petersen *

Department of Chemistry, West Virginia University, Morgantown, WV 26506-6045 (U.S.A.)

(Received August 26th, 1988)

Abstract

The metathetical reaction of $[SiMe_2(C_5H_4)_2]MCl_2$ (M = Ti, Zr) and $[MgCH_2SiMe_2CH_2]_x$ provides a convenient route for the preparation of the corresponding group 4 ansa-metallocenes, $[SiMe_2(C_5H_4)_2]\overline{M(CH_2SiMe_2CH_2)}$ (M = Ti, Zr). These 1-sila-3-metallacyclobutanes have been characterized by elemental analysis, ^1H and ^{13}C NMR measurements, and X-ray diffraction methods. From a comparison with the corresponding structural parameters of the unbridged species, $(C_5H_5)_2\overline{M(CH_2SiMe_2CH_2)}$, the introduction of the $SiMe_2$ bridge results in a 7–10° increase in the dihedral angle between the cyclopentadienyl rings and does not significantly modify the structural paramters within the essentially planar 1-sila-3-metallacyclobutane ring.

Introduction

Metallacyclobutanes of group 4 elements constitute an important class of electrophilic organometallic reagents. Titanacyclobutanes obtained from the cycloaddition of an olefin to Tebbe's reagent, $Cp_2Ti(\mu\text{-}CH_2)(\mu\text{-}Cl)AlMe_2$, have been developed by Grubbs and coworkers as olefin metathesis catalysts [1], as stoichiometric methylene transfer reagents in Wittig-type olefination reactions [2], and most recently as highly-effective catalysts for the ring-opening metathesis polymerization of a broad range of cyclic olefins [3]. Erker and coworkers [4] have observed that the corresponding hafnacyclobutane complex, $Cp_2\overline{Hf(CH_2CH_2CH_2)}$ is accessible by a methylene transfer from the phosphorus ylide, $PPh_3{=}CH_2$, to a reactive (η^2-olefin) hafnocene complex generated during the thermolysis of $Cp_2\overline{Hf(CH_2CH_2CH_2CH_2)}$. Alternatively, the nucleophilic addition of the 1,3-propanediyl dianion, $C_3H_6^{2-}$, to a metallocene dichloride, Cp_2MCl_2 (M = Ti, Zr, and Hf) has been employed by

0022-328X/89/$03.50

Bickelhaupt and coworkers [5] for the preparation of the corresponding metallacyclobutanes, $Cp_2M(CH_2CH_2CH_2)$.

In general, the thermal stability of these metallacyclobutane complexes is dictated by the equilibrium constant associated with the interconversion between the metallacyclobutane and the corresponding metal carbene-olefin species. Grubbs and Straus [6] further observed from studies of a series of alkyl-substituted titanacyclobutanes that steric interactions are important in controlling the stability of these metallacycles. We have since discovered that the thermal stability of these group 4 metallacyclobutanes can be greatly enhanced by placing a Si-atom in the β-position of the four-membered ring. The synthesis of the corresponding 1-sila-3-metallacyclobutane complexes is accomplished by the metathetical reaction of the 1,3-diylmagnesium reagent, $[MgCH_2SiMe_2CH_2]_x$, with the corresponding metallocene dihalides [7]. Subsequent reactivity studies have shown that the 1-sila-3-zirconacyclobutane complexes, $(C_5R_5)_2Zr(CH_2SiMe_2CH_2)$ (R = H, Me) provide suitable electrophilic reagents for investigating the chemistry associated with the insertion of aldehydes [8], CO [9], CO_2 [10], and isonitriles [11] into the Zr–C bond(s) of the saturated zirconacyclobutane ring. As an extension of our ongoing investigations of the chemical behavior of these 1-sila-3-metallacyclobutane complexes, we have prepared the *ansa*-metallocene analogs, $[SiMe_2(C_5H_4)_2]M(CH_2SiMe_2CH_2)$ (M = Ti, Zr), in which the cyclopentadienyl rings are linked by a dimethylsilyl bridge. The presence of an interannular bridge not only reduces the ability of the cyclopentadienyl rings to migrate across the frontier orbital surface of the metal, but can significantly influence the degree of ring canting in these modified-metallocenes [12–14]. In this paper, we wish to describe the synthesis and characterization of $[SiMe_2(C_5H_4)_2]M(CH_2SiMe_2CH_2)$ (M = Ti, Zr). The outcome of X-ray structural studies has provided an opportunity to evaluate the effect of the interannular bridge on the molecular geometry of these modified 1-sila-3-metallacyclobutane complexes.

Experimental

General considerations

All operations were performed under vacuum or a prepurified nitrogen atmosphere on a double-manifold, high-vacuum line or in a Vacuum Atmospheres dry box. Solvents were prepurified by using standard methods and vacuum distilled into storage flasks containing $[(\eta^5\text{-}C_5H_5)_2Ti(\mu\text{-}Cl)_2]_2Zn$ [15] prior to use. All glassware was oven dried overnight prior to use. $[SiMe_2(C_5H_4)_2]MCl_2$ (M = Ti, Zr) [13a,16], and $[MgCH_2SiMe_2CH_2]_x$ [7] were prepared by literature methods.

^1H and ^{13}C NMR spectra were recorded on a JEOL GX-270 spectrometer operating in the FT mode at 270 MHz (^1H) and 67.5 MHz (^{13}C). The spectra were measured in C_6H_6-d_6 using the residual ^1H resonance (δ 7.15 relative to Me_4Si) and the ^{13}C resonance (δ 128.0 relative to Me_4Si) of the solvent as internal standards. Elemental analyses were performed by Dornis and Kolbe Microanalytical Laboratories, Mülheim, West Germany.

Preparation of $[SiMe_2(C_5H_4)_2]M(CH_2SiMe_2CH_2)$ (M = Ti, Zr)

These group 4 metallacyclic complexes are conveniently prepared by the metathetical reaction of $[SiMe_2(C_5H_4)_2]MCl_2$ and $[MgCH_2SiMe_2CH_2]_x$ using the following general procedure. To a 100 ml flask fitted with a solv-seal joint, 1.2 g of

$[SiMe_2(C_5H_4)_2]MCl_2$ and a 10% molar excess of $[MgCH_2SiMe_2CH_2]_x$ are added. The flask is then connected to a pressure-equalizing fritted filter assembly and evacuated. Approximately 50 ml of THF is transferred via vacuum distillation into the reaction vessel. Upon warming to room temperature, the reaction mixture is stirred for several hours. The THF is then removed and an equal volume of pentane is vacuum transferred onto the residue. After filtration, slow removal of the solvent from the pentane solution gives red-orange crystals of $[SiMe_2(C_5H_4)_2]$-$Ti(CH_2SiMe_2CH_2)$ and bright yellow crystals of $[SiMe_2(C_5H_4)_2]Zr(CH_2SiMe_2CH_2)$ in good yield.

$[SiMe_2(C_5H_4)_2]Ti(CH_2SiMe_2CH_2)$. ^{1}H NMR spectrum ($C_6H_6$-$d_6$) δ 6.41 (proximal CH, t, J(H–H) 2.3 Hz), 5.45 (distal CH, t, J(H–H) 2.3 Hz), 2.62 (CH_2, s), 0.15, 0.09 (CH_3, s); gated nondecoupled ^{13}C NMR spectrum (mult, ^1J(C–H) in Hz): δ 122.07, 111.62 (distal and proximal carbons of C_5H_4, dq, 172, 172), 98.95 (bridgehead C, s), 70.96 (CH_2, t, 131), 1.28 ($SiCH_3$, q, 120), −5.55 (bridging $SiCH_3$, q, 122). Anal. Found: C, 59.65; H, 7.86. $C_{16}H_{24}TiSi_2$ calcd.: C, 59.97; H, 7.56%.

$[SiMe_2(C_5H_4)_2]Zr(CH_2SiMe_2CH_2)$. ^{1}H NMR spectrum ($C_6H_6$-$d_6$) δ 6.29 (proximal CH, t, J(H–H) 2.3 Hz), 5.60 (distal CH, t, J(H–H) 2.3 Hz), 1.61 (CH_2, s), 0.26, 0.22 (CH_3, s); gated nondecoupled ^{13}C NMR spectrum (mult, ^1J(C–H) in Hz): δ 119.41, 111.33 (distal and proximal carbons of C_5H_4, dm, 172, 172), 101.27 (bridgehead C, s), 46.15 (CH_2, t, 127), 2.09 ($SiCH_3$, q, 118), −5.03 (bridging $SiCH_3$, t, 121). Anal. Found: C, 52.74; H, 6.65. $C_{16}H_{24}ZrSi_2$ calcd.: C, 52.83; H, 6.65%.

X-Ray data collection

The same general procedures were employed to collect the X-ray diffraction data for $[SiMe_2(C_5H_4)_2]M(CH_2SiMe_2CH_2)$, M = Ti, Zr. Each crystal was sealed in a glass capillary tube under a prepurified N_2 atmosphere and then was transferred to a Picker goniostat which is operated by the computer control of a Krisel Control diffractometer automation system. A preliminary search for low-angle reflections (2θ 5–10°) provided a sufficient number of reflections in each case to use an autoindexing routine [17*] to determine the lattice parameters of the reduced unit cell. From the unrefined orientation matrix, the orientation angles (ω, χ, and 2θ) for 20 higher order reflections were calculated, optimized by the automatic peak-centering algorithm [18*] and least-squares fit to provide the corresponding refined lattice parameters in Table 1 and the orientation matrix.

Intensity data were measured with Zr-filtered Mo-K_α X-ray radiation ($\lambda(K_{\alpha_1})$ 0.70926 Å, $\lambda(K_{\alpha_2})$ 0.71354 Å) at a take-off angle of 2°. Each diffraction peak was scanned at a fixed rate (θ–2θ mode) with the scan width calculated from the expression $w = A + B \tan\theta$. Background counts were measured at the extremes of each scan with crystal and detector kept stationary. The pulse-height analyzer of the scintillation detector was adjusted to accept 90% of the diffracted peak. During data collection the intensities of three standard reflections were measured periodically. The integrated intensity, I, and its standard deviation, $\sigma_c(I)$, for each of the measured peaks were calculated from the expressions $I = w(S/t_s - B/t_b)$ and $\sigma_c(I) = w(S/t_s^2 + B/t_b^2)^{1/2}$, where S represents the total scan count measured in time t_s and B is the combined background count in time t_b. The intensity data were

* Reference numbers with asterisks indicate notes in the list of references.

Table 1

Data for X-ray diffraction analyses of $[SiMe_2(C_5H_4)_2]M(CH_2SiMe_2CH_2)$, M = Ti, Zr

M	Ti	Zr
crystal system	triclinic	triclinic
space group	$P\bar{1}$ (C_i^1, No. 2)	$P\bar{1}$ (C_i^1, No. 2)
a, Å	7.824(4)	12.209(3)
b, Å	10.290(3)	12.449(4)
c, Å	12.935(4)	13.069(6)
α, deg	109.96(2)	66.80(2)
β, deg	102.74(4)	76.45(2)
γ, deg	96.37(4)	83.95(2)
V, Å^3	862.5(6)	1774.6(10)
fw, amu	320.44	363.76
d(calcd), g/cm^3	1.234	1.361
Z	2	4
μ, cm^{-1}	5.92	7.26
crystal dimensions, mm	0.475 × 0.325 × 0.175	0.525 × 0.275 × 0.100
reflections sampled	$\pm hkl(5° \leq 2\theta \leq 45°)$	$\pm h \pm kl(5° \leq 2\theta \leq 45°)$
2θ range for centered reflections	29–34°	25–32°
scan rate	4.0°/min	2.5°/min
scan width, deg	1.1 + 0.8 tan θ	1.1 + 0.8 tan θ
total background time	10 s	16 s
no. of standard reflections	3	3
% crystal decay	4.5%	none
total no. of measured reflections	2399	4898
no. of unique data used	2268 ($F_0^2 \geq 0$)	4654 ($F_0^2 \geq 0$)
agreement between equivalent data		
$R_{av}(F_0)$	0.027	0.034
$R_{av}(F_0^2)$	0.014	0.031
transmission coefficients		0.834–0.930
P	0.03	0.03
discrepancy indices for data with $F_0^2 > \sigma(F_0^2)$		
$R(F_0)$	0.056	0.043
$R(F_0^2)$	0.065	0.051
$R_w(F_0^2)$	0.090	0.070
σ_1	1.44	1.25
no. of variables	244	343
data to parameter ratio	9.3/1	13.6/1

corrected for crystal decay, absorption, and Lorentz-polarization effects. The standard deviation of the square of each structure factor, $F_0^2 = AI/\mathrm{Lp}$, were calculated from $\sigma(F_0^2) = [\sigma_c(F_0^2)^2 + (pF_0^2)^2]^{1/2}$.

Duplicate reflections were averaged. Specific details regarding the lattice parameters and the data collection procedure are summarized in Table 1 for these two compounds.

Structural analyses

Initial coordinates for the Ti and two silicon atoms in $[SiMe_2(C_5H_4)_2]$-$Ti(CH_2SiMe_2CH_2)$ were interpolated from an E-map calculated with the use of MULTAN78 [19] and the phase assignments for the set with the highest figure of merit. The coordinates for the carbon atoms were determined from the subsequent

Fourier summation. After anisotropic refinement of the non-hydrogen atoms, all of the hydrogen atoms were located with difference Fourier techniques utilizing only low-angle data with $(\sin\theta/\lambda) < 0.40$ A^{-1}. Full matrix refinement of the positional and anisotropic thermal parameters for the 19 nonhydrogen atoms and the positional and fixed isotropic thermal parameters for the 24 hydrogen atoms led to final

Table 2

Positional parameters for $[SiMe_2(C_5H_4)_2]\overline{Ti(CH_2SiMe_2CH_2)}$

Atom	x	y	z
Ti	0.00036(9)	0.72979(7)	0.22924(7)
Si1	0.19394(15)	0.97995(11)	0.24199(11)
Si2	−0.23443(16)	0.52011(14)	0.30998(13)
C1	0.0794(6)	0.9500(5)	0.3554(4)
C2	0.1447(6)	0.7989(5)	0.1194(4)
C3	0.1040(8)	1.1081(6)	0.1789(6)
C4	0.4386(7)	1.0474(5)	0.3149(6)
C5	−0.3267(8)	0.3303(7)	0.2291(7)
C6	−0.2891(10)	0.5957(8)	0.4574(7)
C7	0.0085(5)	0.5644(4)	0.3270(4)
C8	0.1290(6)	0.6889(5)	0.4108(4)
C9	0.2722(6)	0.7130(5)	0.3633(5)
C10	0.2450(5)	0.6054(5)	0.2499(5)
C11	0.0828(5)	0.5146(4)	0.2251(4)
C12	−0.2926(5)	0.6180(5)	0.2068(4)
C13	−0.2902(6)	0.7633(6)	0.2446(5)
C14	−0.2642(6)	0.8095(6)	0.1502(6)
C15	−0.2507(6)	0.6948(6)	0.0532(5)
C16	−0.2657(5)	0.5770(5)	0.0863(5)
H1	0.161(5)	0.969(4)	0.428(4)
H2	−0.017(5)	0.993(4)	0.361(4)
H3	0.248(5)	0.770(4)	0.113(4)
H4	0.083(5)	0.795(4)	0.048(4)
H5	0.137(5)	1.197(4)	0.235(4)
H6	−0.021(5)	1.097(4)	0.149(4)
H7	0.161(5)	1.111(4)	0.119(4)
H8	0.461(5)	1.136(4)	0.363(4)
H9	0.492(5)	1.042(4)	0.247(4)
H10	0.489(6)	0.989(4)	0.348(4)
H11	−0.440(5)	0.316(4)	0.218(4)
H12	−0.306(6)	0.285(5)	0.153(4)
H13	−0.268(6)	0.280(4)	0.269(4)
H14	−0.420(5)	0.569(4)	0.436(4)
H15	−0.248(6)	0.684(4)	0.491(5)
H16	−0.246(6)	0.566(5)	0.503(4)
H17	0.121(6)	0.747(4)	0.483(4)
H18	0.365(5)	0.790(4)	0.398(4)
H19	0.321(5)	0.591(4)	0.197(4)
H20	0.039(5)	0.432(4)	0.154(4)
H21	−0.291(6)	0.817(4)	0.318(4)
H22	−0.254(5)	0.901(4)	0.168(4)
H23	−0.235(5)	0.693(4)	−0.022(4)
H24	−0.258(5)	0.485(4)	0.037(4)

Table 3

Positional parameters for $[SiMe_2(C_5H_4)_2]\overline{Zr(CH_2SiMe_2CH_2)}$

Atom	x	y	z
Molecule 1			
Zr	0.25117(3)	0.71708(4)	0.03003(3)
Si1	0.48656(10)	0.76670(11)	−0.02408(10)
Si2	−0.02162(10)	0.67098(12)	0.09108(11)
C1	0.4117(3)	0.6319(4)	0.0842(3)
C2	0.3703(3)	0.8580(4)	−0.0916(3)
C3	0.5506(4)	0.8404(5)	0.0456(5)
C4	0.5954(4)	0.7325(5)	−0.1316(4)
C5	−0.1240(4)	0.7767(5)	0.0175(5)
C6	−0.0873(4)	0.5392(5)	0.2065(4)
C7	0.0965(3)	0.6347(4)	−0.0095(4)
C8	0.1758(4)	0.5420(4)	0.0230(4)
C9	0.2748(4)	0.5656(5)	−0.0625(5)
C10	0.2595(4)	0.6723(5)	−0.1476(4)
C11	0.1527(4)	0.7148(4)	−0.1161(4)
C12	0.0649(3)	0.7427(4)	0.1451(3)
C13	0.1345(3)	0.6812(4)	0.2239(3)
C14	0.2177(4)	0.7558(5)	0.2136(4)
C15	0.2037(4)	0.8617(5)	0.1299(5)
C16	0.1116(4)	0.8558(4)	0.0874(4)
H1	0.4374	0.5623	0.0734
H2	0.4130	0.6229	0.1537
H3	0.3906	0.8654	−0.1658
H4	0.3637	0.9282	−0.0849
H5	0.5967	0.7882	0.0922
H6	0.4966	0.8560	0.0967
H7	0.5924	0.8944	−0.0068
H8	0.6597	0.7002	−0.1081
H9	0.6330	0.8041	−0.1928
H10	0.5607	0.6925	−0.1560
H11	−0.1743	0.8111	0.0716
H12	−0.0857	0.8433	−0.0446
H13	−0.1555	0.7369	−0.0168
H14	−0.1533	0.5605	0.2551
H15	−0.0405	0.4936	0.2595
H16	−0.1244	0.5058	0.1886
H17	0.1676	0.4760	0.0885
H18	0.3468	0.5133	−0.0593
H19	0.3136	0.7097	−0.2204
H20	0.1210	0.7765	−0.1546
H21	0.1323	0.5986	0.2720
H22	0.2700	0.7307	0.2600
H23	0.2457	0.9226	0.1056
H24	0.0817	0.9046	0.0296
Molecule 2			
Zr′	0.74606(3)	0.77408(3)	0.45881(3)
Si1′	0.51861(10)	0.77795(11)	0.43061(12)
Si2′	0.96413(10)	0.78273(11)	0.56235(10)
C1′	0.5689(3)	0.8040(4)	0.5435(4)
C2′	0.6538(4)	0.7530(4)	0.3386(4)
C3′	0.4291(4)	0.6467(5)	0.4966(6)
C4′	0.4402(4)	0.9074(4)	0.3474(4)
C5′	1.1143(4)	0.7623(4)	0.5113(5)

Table 3 (continued)

Atom	x	y	z
Molecule 2			
C6′	0.9350(4)	0.8114(4)	0.6941(4)
C7′	0.8981(3)	0.8973(3)	0.4496(4)
C8′	0.7974(4)	0.9577(4)	0.4701(4)
C9′	0.7502(4)	0.9963(4)	0.3739(5)
C10′	0.8206(5)	0.9620(4)	0.2913(4)
C11′	0.9105(4)	0.8993(4)	0.3378(4)
C12′	0.8795(3)	0.6575(3)	0.5798(3)
C13′	0.7704(3)	0.6284(4)	0.6486(3)
C14′	0.7154(3)	0.5657(4)	0.6071(4)
C15′	0.7880(4)	0.5551(4)	0.5127(4)
C16′	0.8879(3)	0.6117(4)	0.4946(3)
H1′	0.5469	0.8812	0.5463
H2′	0.5431	0.7529	0.6176
H3′	0.6619	0.8114	0.2642
H4′	0.6558	0.6861	0.3341
H5′	0.3703	0.6555	0.5368
H6′	0.4648	0.5732	0.5542
H7′	0.4091	0.6337	0.4484
H8′	0.3795	0.9014	0.3864
H9′	0.4186	0.8863	0.2989
H10′	0.4804	0.9787	0.3201
H11′	1.1455	0.7077	0.5641
H12′	1.1319	0.7294	0.4561
H13′	1.1520	0.8187	0.4964
H14′	0.9405	0.7494	0.7595
H15′	0.8560	0.8348	0.7115
H16′	0.9663	0.8797	0.6837
H17′	0.7597	0.9730	0.5344
H18′	0.6885	1.0378	0.3640
H19′	0.8056	0.9678	0.2154
H20′	0.9755	0.8676	0.2981
H21′	0.7379	0.6483	0.7109
H22′	0.6445	0.5394	0.6388
H23′	0.7704	0.5204	0.4657
H24′	0.9491	0.6184	0.4381

discrepancy indices of $R(F_0) = 0.056$, $R(F_0^2) = 0.065$ and $R_w(F_0^2) = 0.090$ with $\sigma_1 = 1.43$ for the 1855 reflections with $F_0^2 > \sigma(F_0^2)$. A final difference map did not reveal any additional regions of significant electron density.

Approximate positions for the two independent Zr atoms in the asymmetric unit associated with $[SiMe_2(C_5H_4)_2]Zr(CH_2SiMe_2CH_2)$ were interpolated from the first E map calculated on the basis of phases determined by MULTAN78. The coordinates for the remaining nonhydrogen atoms were provided by subsequent Fourier syntheses. All of the hydrogen atoms were eventually located with difference Fourier methods utilizing only low-angle data with $(\sin\theta/\lambda) < 0.40$ Å^{-1}. Full-matrix refinement of the positional and anisotropic thermal parameters for the 38 nonhydrogen atoms with fixed contributions for the 48 hydrogen atoms of the two independent molecules converged with final discrepancy indices of $R(F_0) = 0.043$,

Table 4

Interatomic distances (Å) and bond angles (deg) for non-hydrogen atoms in $[SiMe_2(C_5H_4)_2]$-$M(CH_2SiMe_2CH_2)$, M = Ti, Zr [a]

M	Ti	Zr	
		Molecule 1	Molecule 2
A. Interatomic distances			
M–C1	2.175(4)	2.255(4)	2.253(4)
M–C2	2.148(6)	2.231(4)	2.241(6)
M–C7	2.368(5)	2.483(5)	2.482(5)
M–C8	2.375(5)	2.495(5)	2.500(5)
M–C9	2.426(5)	2.574(7)	2.544(5)
M–C10	2.432(5)	2.571(6)	2.564(4)
M–C11	2.362(5)	2.494(6)	2.489(4)
M–C12	2.363(4)	2.482(4)	2.482(4)
M–C13	2.374(5)	2.490(4)	2.493(4)
M–C14	2.427(5)	2.562(7)	2.555(4)
M–C15	2.430(5)	2.561(7)	2.560(4)
M–C16	2.365(4)	2.500(5)	2.489(4)
Si1–C1	1.868(6)	1.871(4)	1.872(6)
si1–C2	1.869(4)	1.881(4)	1.877(5)
Si1–C3	1.858(7)	1.852(8)	1.853(6)
Si1–C4	1.861(5)	1.843(6)	1.866(5)
Si2–C5	1.833(6)	1.855(5)	1.826(5)
Si2–C6	1.832(9)	1.836(5)	1.841(6)
Si2–C7	1.854(4)	1.859(4)	1.874(4)
Si2–C12	1.855(6)	1.860(6)	1.870(5)
C7–C8	1.404(5)	1.421(6)	1.399(6)
C8–C9	1.397(8)	1.407(6)	1.396(8)
C9–C10	1.379(7)	1.385(7)	1.391(8)
C10–C11	1.398(6)	1.387(7)	1.394(7)
C11–C7	1.425(7)	1.417(5)	1.423(7)
C12–C13	1.403(7)	1.422(6)	1.414(5)
C13–C14	1.408(10)	1.396(8)	1.404(8)
C14–C15	1.375(7)	1.367(7)	1.384(6)
C15–C16	1.398(9)	1.385(8)	1.398(7)
C16–C12	1.425(8)	1.417(6)	1.418(7)
M–Cp1	2.075(6)	2.223(7)	2.216(5)
M–Cp2	2.074(5)	2.221(6)	2.215(4)
B. Bond angles			
C1–M–C2	84.4(2)	81.6(1)	81.2(2)
M–C1–Si1	86.4(2)	87.5(2)	88.0(2)
M–C2–Si1	87.2(2)	88.0(1)	88.2(2)
C1–Si1–C2	102.0(2)	102.8(2)	102.5(2)
C1–Si1–C3	112.3(3)	110.6(2)	109.6(3)
C1–Si1–C4	111.0(3)	111.2(2)	111.6(3)
C2–Si1–C3	111.7(2)	111.7(2)	111.4(3)
C2–Si1–C4	111.7(2)	110.1(2)	110.8(2)
C3–Si1–C4	108.1(3)	110.1(3)	110.6(2)
C5–Si2–C6	113.2(4)	113.6(2)	112.5(3)
C5–Si2–C7	112.3(3)	112.6(2)	112.2(2)
C5–Si2–C12	111.6(3)	110.6(3)	112.0(2)
C6–Si2–C7	112.3(3)	111.9(2)	111.5(2)
C6–Si2–Cl2	112.9(3)	110.4(2)	111.0(2)
C7–Si2–C12	93.1(2)	96.6(2)	96.6(2)
Si2–C7–C8	126.7(3)	124.7(3)	125.1(3)
Si2–C7–C11	122.3(3)	125.8(3)	123.6(3)

Table 4 (continued)

M	Ti	Zr	
		Molecule 1	Molecule 2
C11–C7–C8	105.1(4)	104.6(3)	106.0(4)
C7–C8–C9	109.6(4)	109.4(3)	108.8(5)
C8–C9–C10	108.4(4)	107.6(4)	108.8(4)
C9–C10–C11	107.8(5)	108.3(4)	107.2(5)
C10–C11–C7	109.1(3)	110.1(4)	109.1(4)
Si2–C12–C13	126.2(4)	124.1(3)	125.4(4)
Si2–C12–C16	122.9(4)	126.6(3)	124.0(3)
C16–C12–C13	105.3(5)	104.5(4)	105.2(4)
C12–C13–C14	109.4(5)	109.1(4)	109.3(4)
C13–C14–C15	108.0(5)	108.2(5)	108.0(4)
C14–C15–C16	108.2(6)	108.6(5)	107.9(5)
C15–C16–C12	109.1(4)	109.6(4)	109.5(4)
Si1 · · · M · · · Si2	158.8(1)	177.7(1)	162.2(1)
Cp1 · · · M · · · Cp2	129.8(2)	127.0(2)	126.2(2)

[a] Cp1 and Cp2 denote centroids of the five-membered rings within the dimethylsilyl-bridged bis(cyclopentadienyl) ligand.

$R(F_0^2) = 0.051$, and $R_w(F_0^2) = 0.070$ with $\sigma_1 = 1.25$ for the 3899 data with $F_0^2 > \sigma(F_0^2)$. A final difference map verified the correctness of the structural analysis.

The least-squares refinements of the X-ray diffraction data for both compounds were based on the minimization of $\Sigma\omega_i \mid F_0^2 - S^2F_c^2 \mid^2$ where the individual weight factor, ω_i, is equal to $1/\sigma^2(F_0^2)$ and S is the scale factor. The discrepancy indices were calculated from the expressions $R(F_0) = [\Sigma \mid\mid F_0 \mid - \mid F_c \mid\mid / \Sigma \mid F_0 \mid]$, $R(F_0^2) = \Sigma \mid F_0^2 - F_c^2 \mid / \Sigma F_0^2$, and $R_w(F_0^2) = [\Sigma w_i \mid F_0^2 - F_c^2 \mid / \Sigma w_i F_0^4]^{1/2}$. The "goodness-of-fit" parameter, σ_1, was computed from $\sigma_1 = [\Sigma w_i \mid F_0^2 - F_c^2 \mid^2/(n-p)]^{1/2}$, where n is the number of observations and p is the number of parameters varied during the last refinement cycle. The scattering factors utilized in all of the structure factor calculations were those of Cromer and Mann [20] for the nonhydrogen atoms and those of Stewart et al. [21] for the hydrogen atoms with corrections included for anomalous dispersion effects [22].

The positional parameters from the last least-squares refinement cycle are provided in Tables 2 and 3 for $[SiMe_2(C_5H_4)_2]\overline{Ti(CH_2SiMe_2CH_2)}$ and for $[SiMe_2(C_5H_4)_2]\overline{Zr(CH_2SiMe_2CH_2)}$, respectively. The corresponding interatomic distances and bond angles and the esd's, which were calculated from the estimated standard errors of the fractional atom coordinates are compared in Table 4 for the non-hydrogen atoms. Tables of thermal parameters, pertinent least-squares planes and their dihedral angles, and the observed and calculated structure factors can be obtained upon request. The computer programs that were employed in the crystallographic analyses have been described previously [23].

Results and discussion

The metathetical reaction of $[SiMe_2(C_5H_4)_2]MCl_2$ (M = Ti, Zr) and $[MgCH_2SiMe_2CH_2]_x$ proceeds with the formation of the corresponding *ansa*-metallocene complexes containing a 1-sila-3-metallacyclobutane ring. These compounds

readily sublime under high-vacuum and show no indication of decomposition in benzene solution over an extended period of time. Their ^1H NMR spectra exhibit two pseudo-triplets, which are characteristic of the distal and proximal protons of the $SiMe_2$-bridged bis(cyclopentadienyl) ligand [3,24], and individual singlets for the methylene and two chemically-inequivalent dimethylsilyl groups. Their corresponding ^{13}C $\{^1H\}$ NMR spectra contain three distinct resonances for the bridged cyclopentadienyl rings. The bridgehead carbon resonance is identified by its low intensity and is shifted farthest upfield. As previously observed for $(C_5H_5)_2M(CH_2SiMe_2CH_2)$ [7], the resonances for the methylene carbon in the 1-sila-3-titanacyclobutane complex is shifted ca. 25 ppm downfield from that in the spectrum of the corresponding zirconium compound. Finally, the ^{13}C resonances for the two different silyl-methyl groups can be differentiated by noting that in the ^{13}C NMR spectra of $[SiMe_2(C_5H_4)_2]MCl_2$ [13a] the ^{13}C resonance of the bridging dimethylsilyl group is consistently found 5–6 ppm upfield from TMS.

Description of the Molecular Structures of $[SiMe_2(C_5H_4)_2]M(CH_2SiMe_2CH_2)$, M = Ti, Zr

The molecular structures of $[SiMe_2(C_5H_4)_2]M(CH_2SiMe_2CH_2)$ (M = Ti, Zr) have been determined by X-ray diffraction methods. Although these structurally-similar compounds crystallize in the same triclinic space group, their crystal morphologies are different. For $[SiMe_2(C_5H_4)_2]Ti(CH_2SiMe_2CH_2)$ only one molecule is present in the crystallographic asymmetric unit, whereas for the zirconium analogue two molecules exhibiting different orientations of the $[SiMe_2(C_5H_4)_2]^{2-}$ ligand are present. A perspective view of the overall structure of these 1-metalla-3-silacyclobutane derivatives is shown in Fig. 1 with the corresponding numbering scheme. The pseudo-tetrahedral environment about the central metal atom is comparable to that observed for numerous bent group 4 metallocene complexes [25].

A comparison of the pertinent structural data summarized in Table 5 for $(C_5H_5)_2M(CH_2SiMe_2CH_2)$ and $[SiMe_2(C_5H_4)_2]M(CH_2SiMe_2CH_2)$ reveals that the

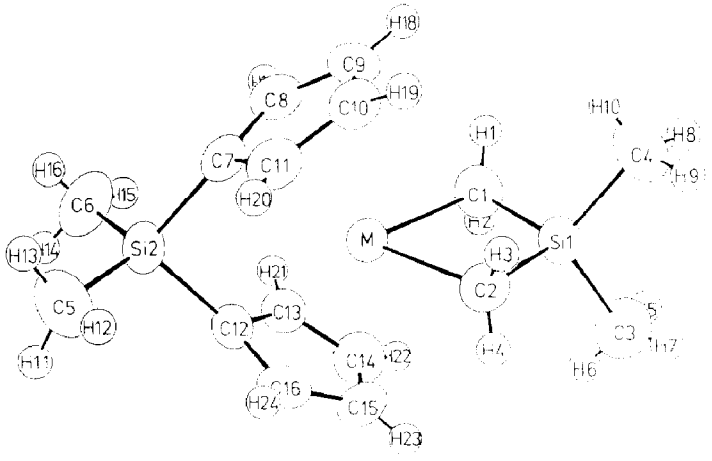

Fig. 1. Perspective view of the molecular configuration of $[SiMe_2(C_5H_4)_2]M(CH_2SiMe_2CH_2)$, M = Ti, Zr with the atom numbering scheme. The thermal ellipsoids are scaled to enclose 50% probability. The radii of the spheres for the hydrogen atoms are arbitrarily reduced for clarity.

Table 5

Pertinent interatomic distances (Å) and bond angles (deg) for $(C_5H_5)_2\overline{M(CH_2SiMe_2CH_2)}$ and $[SiMe_2(C_5H_4)_2]\overline{M(CH_2SiMe_2CH_2)}$ (M = Ti, Zr)

M	$(C_5H_5)_2\overline{M(CH_2SiMe_2CH_2)}$		$[SiMe_2(C_5H_4)]\overline{M(CH_2SiMe_2CH_2)}$		
	Ti	Zr	Ti	Zr(molecule 1)	Zr(molecule 2)
M–C	2.146(3)	2.240(5)	2.175(4)	2.255(4)	2.253(4)
			2.148(6)	2.231(4)	2.241(6)
C–Si	1.863(3)	1.833(3)	1.868(6)	1.871(4)	1.872(6)
			1.869(4)	1.881(4)	1.877(5)
Si–MeC	1.872(8)	1.858(9)	1.858(7)	1.852(8)	1.853(6)
	1.868(5)	1.865(6)	1.861(5)	1.843(6)	1.866(5)
M · · · Cp	2.088(3)	2.223(4)	2.075(6)	2.223(7)	2.216(5)
	2.084(6)	2.231(11)	2.074(5)	2.221(6)	2.215(4)
C–M–C	84.1(2)	81.0(2)	84.4(2)	81.6(1)	81.2(2)
Cp · · · M · · · Cp	132.9(2)	132.8(2)	129.8(2)	127.0(2)	126.2(2)
M–C–Si	87.2(1)	88.3(2)	86.4(2)	87.5(2)	88.0(2)
			87.2(2)	88.0(1)	88.2(2)
C–Si–C	101.0(2)	102.2(3)	102.0(2)	102.8(2)	102.5(2)
MeC–Si–MeC	109.7(3)	110.0(3)	108.1(3)	110.1(3)	110.6(2)
Pucker angle	7.7	4.7	0.2	2.8	2.1

dimethylsilyl bridge does not significantly modify the structure of the 1-sila-3-metallacyclobutane ring. The M–C and C–Si bond distances and C–M–C, M–C–Si, and C–Si–C bond angles within each of the appropriate pairs of metallacyclic rings are equivalent within experimental error. Whereas the solid-state structures of $(C_5H_5)_2\overline{M(CH_2SiMe_2CH_2)}$ are each constrained by a crystallographic mirror plane, the structures of $[SiMe_2(C_5H_4)_2]\overline{M(CH_2SiMe_2CH_2)}$ are well-behaved and free of any crystallographically-imposed symmetry. For all practical purposes, the MC_2Si rings are essentially planar. The folding of the MC_2Si ring along the C · · · C vector in these 1-sila-3-metallacyclobutane complexes is comparable to the corresponding puckering angles of 5.8° in $(C_5H_5)_2\overline{Th(CH_2SiMe_2CH_2)}$ [26] and 3.25° in $(C_5H_5)_2\overline{Ti(CH_2CH(C_6H_5)CH_2)}$ [27]. The small observed variation in this parameter is probably a consequence of crystal packing effects.

The replacement of the two C_5H_5 rings by the dimethylsilyl-bridged bis(cyclopentadienyl) ligand causes an increase in the canting of the cyclopentadienyl rings.

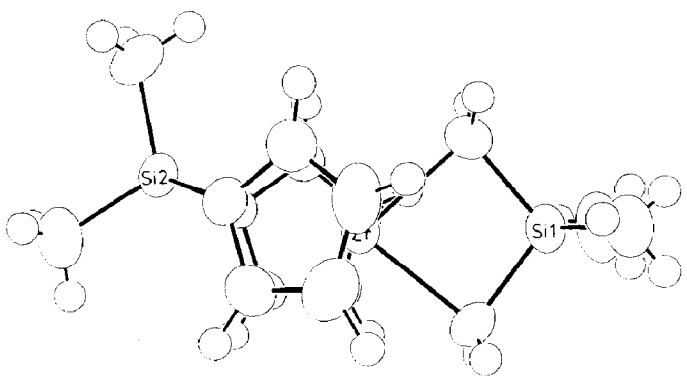

Fig. 2. Top view of molecule 2 of $[SiMe_2(C_5H_4)_2]\overline{Zr(CH_2SiMe_2CH_2)}$ depicting lateral rotation of dimethylsilyl-bridged bis(cyclopentadienyl) ligand.

The magnitude of this structural effect is illustrated best by comparing the dihedral angles between the planes of the cyclopentadienyl rings in the corresponding unbridged and bridged complexes. For the 1-sila-3-titanacyclobutane complexes, this angle increases by ca. 7° from 48.3° in $(C_5H_5)_2Ti(CH_2SiMe_2CH_2)$ to 55.0° in $[SiMe_2(C_5H_4)_2]Ti(CH_2SiMe_2CH_2)$. For the respective 1-sila-3-zirconacyclobutane complexes, this angle increases by 10° from 49.0° to an averaged value of 59.0°. By opening the wedge defined by the cyclopentadienyl rings, the electron-deficient metal in these *ansa*-metallocenes should be more accessible to nucleophilic attack. Comparative reactivity studies are planned to determine whether or not this structural variation produces a significant enhancement in the rate of insertion into the M–C bond.

Another interesting structure feature associated with $[SiMe_2(C_5H_4)_2]M(CH_2SiMe_2CH_2)$ is the orientation of the ring-bridged bis(cyclopentadienyl) ligand. Previous structural studies of $[SiMe_2(C_5H_4)_2]MCl_2$ [13a,14] indicated that the dimethylsilyl linkage is disposed symmetrically with the molecule lying on a crystallographic two-fold rotation axis which bisects the Cl–M–Cl angle. If this structural arrangement were maintained for the corresponding 1-sila-3-metallacyclobutane derivatives, then the Si2 · · · M · · · Si1 angle should be 180°. For molecule 1 of $[SiMe_2(C_5H_4)_2]Zr(CH_2SiMe_2CH_2)$, this angle is 177.7°. However, for $[SiMe_2(C_5H_4)_2]Ti(CH_2SiMe_2CH_2)$ and molecule 2 of $[SiMe_2(C_5H_4)_2]Zr(CH_2SiMe_2CH_2)$, the ring-bridged ligand is rotated laterally by ca. 20° such that the respective Si2 · · · M · · · Si1 angles are 158.8° and 162.2°. Figure 2 provides an alternate view (along the normal to the ZrC_2Si ring in molecule 2) which depicts the lateral displacement of the $SiMe_2$ bridge. Despite this structural alteration, the cyclopentadienyl rings remain eclipsed and the bridging Si atom resides on the MC_2 plane that bisects the dihedral angle of the planar cyclopentadienyl rings.

Acknowledgements

Support for this research was provided by the West Virginia Energy Research Center and the donors of the Petroleum Research Fund as administered by the American Chemical Society. Computer time for the X-ray diffraction data analyses was provided by the West Virginia Network for Educational Telecomputing.

References

1 (a) T.R. Howard, J.B. Lee, and R.H. Grubbs, J. Am. Chem. Soc., 12 (1980) 6876; (b) J.B. Lee, K.C. Ott, and R.H. Grubbs, ibid., 104 (1982) 7491.
2 K.A. Brown-Wensley, S.L. Buchwald, L. Cannizzo, L. Clawson, S. Ho, D. Meinhardt, J.R. Stille, D. Straus, and R.H. Grubbs, Pure Appl. Chem., 55 (1983) 1733.
3 (a) L.R. Gilliom and R.H. Grubbs, J. Am. Chem. Soc., 108 (1986) 733; (b) T.M. Swager and R.H. Grubbs, ibid., 109 (1987) 894.
4 G. Erker, P. Czisch, C. Krüger, and J.M. Wallis, Organometallics, 4 (1985) 2059.
5 (a) J.W.F.L. Seetz, F.A. Hartog, H.P. Bohm, C. Blomberg, O.S. Akkerman, and F. Bickelhaupt, Tetrahedron Lett., 23 (1982) 1497; (b) J.W.F.L. Seetz, G. Schat, O.S. Akkerman, and F. Bickelhaupt, J. Am. Chem. Soc., 104 (1982) 6848; (c) J.W.F.L. Seetz, G. Schat, O.S. Akkerman, and F. Bickelhaupt, Angew. Chem., 95 (1983) 242.
6 D.A. Straus and R.H. Grubbs, Organometallics, 1 (1982) 1658.
7 W.R. Tikkanen, J.Z. Liu, J.W. Egan, Jr., and J.L. Petersen, Organometallics, 3 (1984) 825.
8 W.R. Tikkanen and J.L. Petersen, Organometallics, 3 (1984) 1651.

9 J.L. Petersen and J.W. Egan, Jr., Organometallics, 6 (1987) 2007.
10 J.L. Petersen and J.W. Egan, Jr., unpublished results.
11 F.J. Berg and J.L. Petersen, manuscript in preparation.
12 (a) J.A. Smith, J. von Seyerl, G. Huttner, and H.H. Brintzinger, J. Organomet. Chem., 173 (1979) 175; (b) J.A. Smith and H.H. Brintzinger, ibid., 218 (1981) 159.
13 (a) C.S. Bajgur, W.R. Tikkanen, and J.L. Petersen, Inorg. Chem., 24 (1985), 2539 and references cited therein. The references given in Table VII of this paper were numbered wrong and can be corrected by adding two to each reference number; (b) C.S. Bajgur, S.B. Jones, and J.L. Petersen, Organometallics, 4 (1985) 1929.
14 H. Köpf and J. Pickardt, Z. Naturforsch. B, 36 (1981) 1208.
15 D.G. Sekutoski and G.D. Stucky, J. Chem. Educ., 53 (1976) 110.
16 H. Köpf and W. Kahl, J. Organomet. Chem., 64 (1974) C37.
17 The automatic reflection-indexing algorithm is based upon Jacobson's procedure: R.A. Jacobson, J. Appl. Crystallogr., 9 (1976) 115.
18 The automatic peak-centering algorithm is similar to that described by Busing: W.R. Busing, in F.R. Ahmed (Ed.), Crystallographic Computing, Munksgaard, Copenhagen, 1970 p. 319. The ω, χ, and 2θ angles are optimized with respect to the K_{α_1} peak (λ 0.70926 Å).
19 J.P. Declerq, D. Germain, P. Main and M.M. Woolfson, Acta Crystallogr., Sect. A., A29 (1973) 231.
20 D.T. Cromer and J. Mann, J. Acta. Crystallogr., Sect. A, A24 (1968) 231.
21 R.F. Stewart, E.R. Davidson and W.T. Simpson, J. Chem. Phys., 42 (1965) 3175.
22 D.T. Cromer and D.J. Liberman, J. Chem. Phys., 53 (1970) 1891.
23 J.L. Petersen, J. Organomet. Chem., 155 (1979) 179.
24 H. Köpf and N. Klouras, Z. Naturforsch. B, 38 (1983) 321.
25 (a) M. Bottrill, P.D. Gavens, J.W. Kelland, and J. McMeeking, G. Wilkinson, F.G.A. Stone, and E.W. Abel (Eds.), Comprehensive Organometallic Chemistry, Pergamon Press, Oxford (1982) 271; (b) D.J. Cardin, M.F. Lappert, C.L. Raston, and P.I. Riley, ibid., p. 549.
26 J.W. Bruno and T.J. Marks, J. Am. Chem. Soc., 104 (1982) 7357.
27 J.B. Lee, G.J. Gajda, W.P. Schaefer, T.R. Howard, T. Ikariya, D.A. Straus, and R.H. Grubbs, J. Am. Chem. Soc., 103 (1981) 7358.